

Invited, Review

Surface Sensitivity of Auger-Electron Spectroscopy and X-ray Photoelectron Spectroscopy

C. J. Powell^{1*} and A. Jablonski²

¹Surface and Microanalysis Science Division, National Institute of Standards and Technology, Gaithersburg, MD 20899-8370, USA

²Institute of Physical Chemistry, Polish Academy of Sciences, ul. Kasprzaka 44/52, 01-224 Warsaw, Poland
*cedric.powell@nist.gov

(Received: October 4, 2010; Accepted: January 6, 2011)

Four terms are commonly used as measures of the surface sensitivity of Auger electron spectroscopy (AES) and X-ray photoelectron spectroscopy (XPS): the inelastic mean free path (IMFP), the effective attenuation length (EAL), the mean escape depth (MED), and the information depth (ID). These terms have been defined by the International Organization for Standardization (ISO) and ASTM International, and are utilized in various ISO standards. The IMFP, EAL, MED, and ID are intended for different applications. We give information on sources of data for IMFPs, EALs, and MEDs, and present simple analytical expressions from which IMFPs, EALs, MEDs, and IDs can be determined.

1. Introduction

Auger-electron spectroscopy (AES), secondary-ion mass spectrometry (SIMS), and X-ray photoelectron spectroscopy (XPS) are in common use for surface analysis. Figure 1 shows the numbers of published AES, SIMS, and XPS papers published per year from 1991 through 2009 based on a key word search [1]. Two sets of AES publication data are included in Fig. 1, one based on the use of 'AES' in the search and the other without this term. The former data set is an overcount (because AES is also an abbreviation for atomic emission spectroscopy), while the latter data set is an undercount (since some Auger papers with AES in the title or abstract would be missed). Nevertheless, it appears from Fig. 1 that the number of Auger papers is roughly constant or slowly decreasing while the number of SIMS papers is slowly increasing. There is a much larger growth in the number of XPS papers, probably due to the fact that XPS has been successfully applied to many different types of materials [2]. The plots in Fig. 1 do not, of course, show the many unpublished practical applications of each technique nor the economic impacts of these applications. Nevertheless, Fig. 1 indicates that XPS applications are of growing significance.

Four terms are in common use as measures of the surface sensitivity of AES and XPS: the inelastic mean free path (IMFP), the effective attenuation length (EAL), the mean escape depth (MED), and the information depth (ID). Misunderstandings often

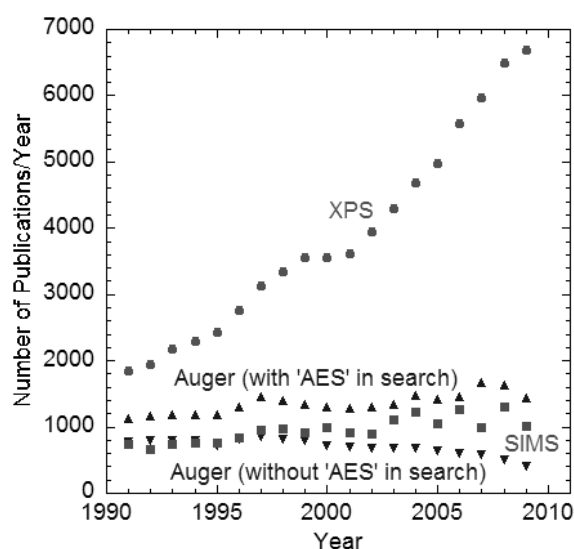


Fig. 1. Plot of numbers of papers published per year on AES, SIMS, and XPS from 1991 through 2009 based on a web search using abbreviations and key phrases for these techniques [2].

arise if these terms are not used correctly since each has a separate definition [3,4]. Another complicating factor that is sometimes overlooked is elastic scattering of the signal electrons. Values of the EAL, MED, and ID depend on the elastic-scattering properties of the sample and, for XPS, on the experimental configuration. A further source of complication is that the EAL can be defined for different applications (e.g., for measuring thicknesses of overlayer films and for quantitative analyses). An EAL value will then depend on the application. Use of the correct term is particularly important when applying a standard from the International Organization for Standardization (ISO) [5].

We give a brief overview of the IMFP, EAL, MED, and ID for AES and XPS. Definitions of each term are given [3,4] together with information on sources of available data. More detailed information can be found in a recent review [6].

2. Inelastic Mean Free Paths

The IMFP has been defined as the average distance that an electron with a given energy travels between successive inelastic collisions [3]. It is a basic material parameter that is utilized in determinations of the EAL, MED, and ID.

Tanuma *et al.* reported IMFPs for groups of elemental solids, inorganic compounds, and organic compounds for energies between 50 eV and 2 keV [7]. These IMFPs were calculated using the full Penn algorithm [8] and experimental optical data. Tanuma *et al.* analyzed their IMFPs for elements and organic compounds to obtain a predictive formula, designated TPP-2M, for the IMFP, λ_{in} , in nm:

$$\lambda_{in} = \frac{E}{10E_p^2[\beta \ln(\gamma E) - (C/E) + (D^*/E^2)]} \quad (1)$$

$$\beta = -0.10 + 0.944(E_p^2 + E_g^2)^{-1/2} + 0.069\rho^{0.1}$$

$$\gamma = 0.191\rho^{-1/2}$$

$$C = 1.97 - 0.91U$$

$$D^* = 53.4 - 20.8U$$

$$U = N_v\rho / A = E_p^2 / 829.4$$

where the electron energy E is expressed in eV, ρ is the density of the solid (in g/cm³), $E_p = 28.8(N_v\rho / A)^{1/2}$ is the free-electron

plasmon energy (in eV), N_v is the number of valence electrons per atom (for elemental solids) or molecule (for compounds), A is the atomic or molecular weight, and E_g is the bandgap energy (in eV) for nonconductors.

Tanuma *et al.* [9] have recently published new calculations of IMFPs for a group of 41 elemental solids over the 50 eV to 30 keV energy range, again using the full Penn algorithm [8] and experimental optical data. An important finding [9] was that Eq. (1) was found to be satisfactory for energies up to 30 keV. The new IMFPs were also found to agree well with IMFPs from recent calculations [10,11] and from elastic-peak electron spectroscopy (EPES) experiments [12,13].

IMFPs have been derived recently by Werner *et al.* for a group of 17 elemental metals from analyses of measured reflection electron energy-loss spectra (REELS) at two well-separated primary energies [14]. Bourke and Chantler have also reported a new method for determining IMFPs at energies between about 5 eV and about 120 eV from analyses of near-edge structure in X-ray absorption spectra (XAS) [15]. Figure 2 shows a comparison of calculated IMFPs for Cu by Tanuma *et al.* [7] with IMFPs from EPES experiments by Tanuma *et al.* [12], IMFPs from REELS by Werner *et al.* [14], and IMFPs from XAS data by Bourke and Chantler [15]. We see that there is good consistency of the calculated IMFPs with IMFPs from EPES and REELS but disagreement with IMFPs from XAS data for energies below 50 eV. This disagreement is not unexpected since the Penn algorithm becomes unreliable at such low energies [7,9].

Near a surface, the probability for bulk inelastic excitations is reduced and there is an increased probability for surface-electronic excitations, particularly for energies less than about 1 keV, more-grazing detection of Auger electrons or photoelectrons, and smooth surfaces [16]. Pauly and Tougaard [17] have recently developed a model to determine the combined effects of surface excitations and intrinsic excitations on XPS intensities which can together lead to a reduction in the absolute peak intensities of about 35-45 %. The relative changes, however, are only about ± 10 % for emission angles less than 60° and energies less than 1500 eV [17].

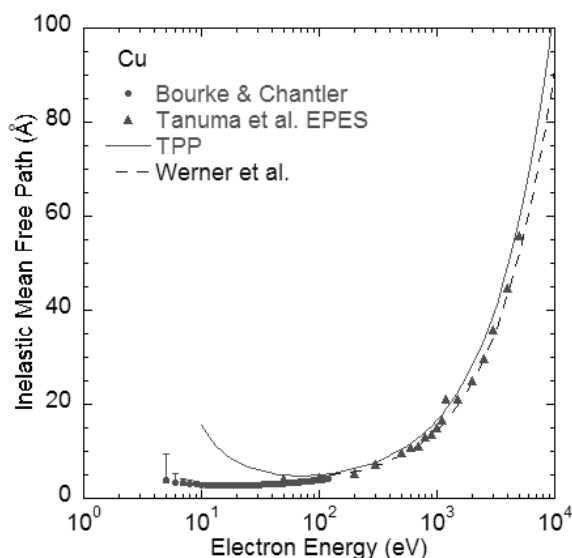


Fig. 2. Comparison of IMFPs calculated from optical data for Cu by Tanuma *et al.* [9] (TPP, solid line) with IMFPs from REELS experiments by Werner *et al.* [14] (dashed line), IMFPs from EPES experiments by Tanuma *et al.* [12] (\blacktriangle), and IMFPs from analyses of XAS data by Bourke and Chantler [15] (\bullet).

IMFPs can be conveniently obtained from a database available from the National Institute of Standards and Technology (NIST) [18]. IMFPs calculated from optical data and values obtained from EPES experiments are available for a limited number of materials. For other materials, IMFPs can be obtained from the TPP-2M equation or another predictive IMFP equation proposed by Gries [19].

3. Effective Attenuation Lengths

The EAL has been defined as the parameter which, when introduced in place of the inelastic mean free path into an expression derived for AES and XPS on the assumption that elastic-scattering effects are negligible for a given quantitative application, will correct that expression for elastic-scattering effects [3]. This definition has two notes that provide additional information. First, the EAL may have different values for different quantitative applications of AES and XPS. However, the most common use of EAL is the determination of overlayer-film thicknesses from measurement of the changes of substrate Auger-electron or photoelectron signal intensities after deposition of a film or as a function of emission angle. For emission angles of up to about 60° (with respect to the surface normal), it is often satisfactory to use a

single value of this parameter. For larger emission angles, the EAL can depend on this angle. Second, since there are different uses of EAL, it is recommended that users specify clearly the particular application and the definition of the parameter for that application (e.g., by giving an equation or by providing a reference to a particular source).

If we ignore (for the moment) the effects of elastic scattering, the intensity of Auger electrons or photoelectrons emitted from a substrate, I_s , covered by a uniform overlayer-film of thickness, t , would be given by

$$I_s = I_s^0 \exp[-t/(\lambda_{in} \cos \alpha)], \quad (2)$$

where I_s^0 is the signal intensity from the bare substrate ($t = 0$), α is the angle of emission of Auger electrons or photoelectrons from the surface (with respect to the surface normal), and λ_{in} is the IMFP for the substrate-signal electrons in the overlayer material. A thickness t could then be calculated from measurements of I_s^0 and I_s and appropriate IMFP data.

Elastic scattering of the signal electrons can be considered simply by replacing the IMFP in Eq. (2) with the EAL. It is convenient to define a “practical” EAL, L , for a specified experimental configuration and a film of particular thickness [20-22]:

$$L = \frac{1}{\cos \alpha} \frac{t}{(\ln I_s^0 - \ln I_s)} \quad (3)$$

or

$$L = \frac{1}{\cos \alpha} \frac{t}{[\ln \int_0^\infty \phi(z, \alpha) dz - \ln \int_t^\infty \phi(z, \alpha) dz]}, \quad (4)$$

where $\phi(z, \alpha)$ is the emission depth distribution function (DDF), a function of depth from the surface, z , and α . Since the DDF is, in general, non-exponential [20], L will be a function of t and α rather than simply a material constant like the IMFP. Values of L for a specified AES or XPS configuration can be obtained from Eq. (3) using measured values of I_s^0 and I_s or from Eq. (4) with a calculated DDF. It is also often convenient to use an average value of L , L_{ave} , for a specified range of film thicknesses when L does not vary significantly with thickness.

We have reported calculations of L for selected photoelectron and Auger-electron lines from a number of elemental solids and compounds [20-24]. These EALs were determined from DDFs obtained from an algorithm based on solution of the kinetic Boltzmann equation within the transport approximation [25]. In this approach, it is assumed that elastic scattering is isotropic and that the corresponding cross section is the so-called transport cross section, given by an integral of the differential elastic-scattering cross section multiplied by $(1 - \cos\theta)$ where θ is the polar scattering angle; the latter factor emphasizes the contributions of large-angle elastic-scattering events to the transport cross section [26]. It is further assumed that the elastic- and inelastic-scattering properties of the substrate and the overlayer film are the same.

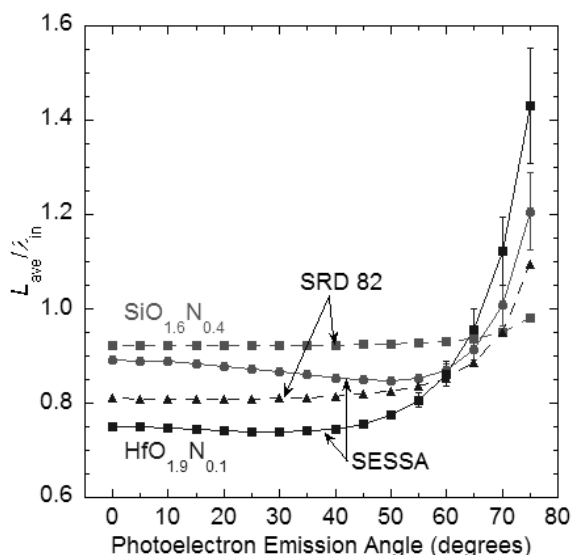


Fig. 3. Ratios of the average EAL, L_{ave} , to the IMFP, λ_{in} , for Si $2p_{3/2}$ photoelectrons in thin films of $\text{SiO}_{1.6}\text{N}_{0.4}$ and $\text{HfO}_{1.9}\text{N}_{0.1}$ on Si [32]. The solid lines show EALs from SESSA [30] and the dashed lines show EALs from SRD 82 [28]. The error bars on the EALs from SESSA indicate one-standard-deviation uncertainties in the fits of Eq. (3) to the simulated photoelectron intensities.

We have found a simple analytical formula for the ratio of L_{ave} to the IMFP, R_{EAL} , from our calculated EALs from Eq. (4) for photoelectron and Auger-electron lines of a group of elemental solids and inorganic compounds (Si, Cu, Ag, W, Au, ZrO_2 , ZrSiO_4 , HfO_2 , and HfSiO_4) [24]. For emission angles between 0° and 50° and for film thicknesses corresponding to attenuation of the substrate intensity to 1 %, 5 %, and 10 % of its maximum value,

$$R_{EAL} = L_{ave} / \lambda_{in} = 1.0 - 0.735\omega, \quad (5)$$

where $\omega = \lambda_{in} / (\lambda_{in} + \lambda_t)$ is the single-scattering albedo, a convenient measure of the strength of elastic scattering, and λ_t is the transport mean free path (TMFP) that can be calculated readily from the transport cross section [24,26]. The average deviation of the R_{EAL} values from the line was 0.61 % [24]. A similar analytical expression for R_{EAL} has been published by Seah and Gilmore [6,27].

The NIST Electron EAL Database (SRD 82) provides values of L and L_{ave} for materials and measurement conditions specified by the user [28]. These EALs are calculated from Eq. (4) which is based on the transport approximation. EALs can also be determined from Eq. (5) or the Seah-Gilmore expression [27].

EALs for the measurement of overlayer-film thicknesses can also be obtained by Monte Carlo simulations [21]. These EALs are expected to be more reliable than those from the transport approximation since elastic- and inelastic-scattering parameters specific to the substrate and overlayer-film materials can be utilized [29]. The NIST Database for the Simulation of Electron Spectra for Surface Analysis (SESSA) provides parameter data for quantitative analyses by AES and XPS and can perform Monte Carlo simulations of AES and XPS spectra for multi-layer thin-film samples and measurement conditions specified by the user [30,31].

The solid lines in Fig. 3 show ratios of average EALs from SESSA to the IMFP for Si $2p_{3/2}$ photoelectrons from a silicon substrate in thin overlayer films of $\text{SiO}_{1.6}\text{N}_{0.4}$ and $\text{HfO}_{1.9}\text{N}_{0.1}$ [32]. These EALs were calculated for 0.5 nm, 1.5 nm, 2.5 nm, 3.5 nm, and 4.5 nm films of each compound for emission angles from 0° to 75° in 5° increments and for XPS with Al $K\alpha$ X-rays and an angle of 55° between the direction of X-rays and the direction of emitted photoelectrons accepted by the analyzer. The dashed lines in Fig. 3 show similar ratios for EALs from SRD 82. We see that there are numerical differences between EALs from the two databases, with the EALs from SESSA expected to be the more reliable.

4. Mean Escape Depths

The MED has been defined as the average depth normal to the surface from which the specified particles or radiation escape, as given by:

$$D = \int_0^{\infty} z\phi(z, \alpha)dz / \int_0^{\infty} \phi(z, \alpha)dz, \quad (6)$$

where $\phi(z, \alpha)$ is the emission depth distribution function (DDF) for depth z from the surface into the material and for angle of emission α with respect to the surface normal [3]. The DDF is defined, for a measured signal of particles or radiation emitted from a surface, as the probability that the particle or radiation leaving the surface in a specified state and in a specified direction originated from a specified depth measured normally from the surface into the material [3].

The MED is a convenient measure of surface sensitivity in AES and XPS since it is a function of both the specimen material and the measurement conditions, particularly the emission angle of the detected electrons. If elastic scattering of the signal electrons is neglected, for the moment, the corresponding MED, Δ , from Eq. (6) is:

$$\Delta = \lambda_{in} \cos \alpha. \quad (7)$$

In general, the effects of elastic scattering cannot be neglected and it is necessary to determine the MED from a calculated DDF in Eq. (6). As for the EAL, the effects of elastic scattering can be conveniently expressed by a ratio, R_{MED} , given by:

$$R_{MED} = D / \Delta. \quad (8)$$

We have reported calculations of R_{MED} for photoelectron and Auger-electron lines of the same group of elemental solids and inorganic compounds discussed in the previous section [24]. These calculations were made, as before, with DDFs obtained from the transport approximation. For emission angles between 0° and 50° , values of R_{MED} did not vary appreciably with α . We found empirically that R_{MED} varied linearly with the single-scattering albedo:

$$R_{MED} = 1.00 - 0.736\omega. \quad (9)$$

The average deviation of individual R_{MED} values from the line was 0.25 % [24].

Equation (9) can be used as a predictive guide for determining MEDs in other materials. Values of the MED are also provided by SRD 82 [28].

5. Information Depths

The ID is a useful measure of the sampling depth in a particular AES or XPS experiment. It has been defined as the maximum depth, normal to the surface, from which useful information is obtained [3]. This definition has three notes that provide additional information. First, the information depths for different surface-analysis methods may differ significantly. The ID for each technique depends on the material being analyzed, the particular signals being recorded from that material, and the instrument configuration. Second, the ID can be identified with the sample thickness from which a specified percentage (e.g., 95 % or 99 %) of the detected signal originates. Finally, the ID may be determined from a measured, calculated, or estimated emission DDF for the signal of interest.

The ID, S , can be determined from a calculated DDF [33]:

$$\frac{\int_0^S \phi(z, \alpha)dz}{\int_0^{\infty} \phi(z, \alpha)dz} = \frac{P}{100}, \quad (10)$$

where P is a selected percentage of the signal intensity from the surface layer. A user can select a value appropriate for an application, but we suggest that percentages of 90 %, 95 %, and 99 % could be useful. Equation (10) cannot be solved analytically with the DDF of Tilinin *et al.* [25]; instead, this equation has to be solved numerically.

If we initially neglect elastic scattering, an analytical expression can be derived for the corresponding ID, Σ [24]:

$$\Sigma = -\lambda_{in} \cos \alpha \ln[1 - (P/100)] \quad (11)$$

As for the EAL and the MED, it is convenient to examine the ratio,

$$R_{ID} = S / \Sigma, \quad (12)$$

to observe the effects of elastic scattering on the ID.

We have performed calculations of R_{ID} for the same group of photoelectron and Auger-electron lines

discussed in the previous two sections and for $P = 90\%$, $P = 95\%$, and $P = 99\%$ [24]. As for R_{EAL} and R_{MED} , R_{ID} was nearly independent of α for $0^\circ \leq \alpha \leq 50^\circ$. In this angular range, R_{ID} also varied linearly with ω :

$$R_{ID} = 1.00 - 0.787\omega. \quad (13)$$

The average deviation of individual R_{ID} values from the line was 0.54 % [24]. Equation (13) can be similarly used to estimate IDs in other materials.

We note here that R_{EAL} from Eq. (5), R_{MED} from Eq. (9), and R_{ID} from Eq. (13) have similar but non-identical linear dependencies on ω . This result is simply due to the fact that the average EAL, the MED, and the ID are derived from different functions of the DDF.

6. Single-Scattering Albedo

The single-scattering albedo, needed for the evaluation of Eqs. (5), (9), and (13), can be obtained from values of the IMFP and TMFP from SRD 82 [28] and SESSA [30]. For energies above about 1 keV, ω decreases monotonically with increasing energy and increases with atomic number, Z [6]. For lower energies, the dependencies on E and Z are more complex [6]. A specific calculation of ω for a given energy and material is needed to determine values of the average EAL [Eq. (5)], the MED [Eq. (9)], and the ID [Eq. (13)].

7. Summary

Current ISO standards require the use of IMFPs, EALs, and MEDs in AES and XPS for quantitative analyses, determination of film thicknesses, and other purposes. Each of these terms and the ID has a different definition, and data intended for one application should not be used for another. In addition, different EALs exist for different purposes (i.e., in different analytical equations).

We have provided a summary of available data for the IMFP, EAL, MED, and ID. NIST databases provide values for IMFPs [18], EALs [28,30], and MEDs [28]. Analytical expressions are available for IMFPs and, for electron emission angles between 0° and 50° , also for EALs, MEDs, and IDs. EALs from Monte Carlo simulations (e.g., with SESSA [30]) are expected to be

more reliable than those from the transport approximation (e.g., from SRD 82 [28]).

8. References

- [1] Web of Science, Institute for Scientific Information, Philadelphia, Pennsylvania.
- [2] C. J. Powell, J. Vac. Sci. Technol. A 21, S42 (2003).
- [3] ISO 18115, *Surface Chemical Analysis – Vocabulary*, International Organisation for Standardisation, Geneva (2001); ISO 18115, *Surface Chemical Analysis – Vocabulary – Amendment 2*, International Organisation for Standardisation, Geneva (2007).
- [4] ASTM E673-03, Standard Terminology Relating to Surface Analysis, Annual Book of ASTM Standards 2010, Vol. 3.06, ASTM International, West Conshohocken, 2010, p. 655.
- [5] See <http://www.iso.org>.
- [6] C. J. Powell and A. Jablonski, Nucl. Instr. Methods in Phys. Res. A 601, 54 (2009).
- [7] S. Tanuma, C. J. Powell, and D. R. Penn, Surf. Interface Anal. 21, 165 (1994).
- [8] D. R. Penn, Phys. Rev. B 35, 482 (1987).
- [9] S. Tanuma, C. J. Powell, and D. R. Penn, Surf. Interface Anal. (in press).
- [10] S. F. Mao, Y. G. Li, R. G. Zeng, and Z. J. Ding, J. Appl. Phys. 104, 114907 (2008); *ibid.* 105, 099902 (2005).
- [11] C. D. Denton, I. Abril, R. Garcia-Molina, J. C. Moreno-Marin, and S. Heredia-Avalos, Surf. Interface Anal. 40, 1481 (2008).
- [12] S. Tanuma, T. Shiratori, T. Kimura, K. Goto, S. Ichimura, and C. J. Powell, Surf. Interface Anal. 37, 833 (2005).
- [13] W. S. M. Werner, C. Tomastik, T. Cabela, G. Richter, and H. Störi, J. Electron Spectrosc. Relat. Phenom. 113, 127 (2001).
- [14] W. S. M. Werner, K. Glantschnig, and C. Ambrosch-Draxl, J. Phys. Chem. Ref. Data 38, 1013 (2009).
- [15] J. D. Bourke and C. T. Chantler, Phys. Rev. Letters 104, 206601 (2010).
- [16] C. J. Powell and A. Jablonski, J. Electron Spectrosc. Relat. Phenom. 178-179, 331 (2010).
- [17] N. Pauly and S. Tougaard, Surf. Science 604,

- 1193 (2010).
- [18] C. J. Powell and A. Jablonski, NIST Electron Inelastic-Mean-Free-Path Database, SRD 71, Version 1.1 (2000); <http://www.nist.gov/ts/msd/srd/nist71.cfm>.
- [19] W. H. Gries, Surf. Interface Anal. 24, 38 (1996).
- [20] A. Jablonski and C. J. Powell, Surf. Science Reports 47, 33 (2002).
- [21] C. J. Powell and A. Jablonski, Surf. Interface Anal. 33, 211 (2002).
- [22] A. Jablonski and C. J. Powell, J. Alloys Compounds 362, 26 (2004).
- [23] C. J. Powell and A. Jablonski, J. Vac. Sci. Technol. A 19, 2604 (2001).
- [24] A. Jablonski and C. J. Powell, J. Vac. Sci. Technol. A 27, 253 (2009).
- [25] I. S. Tilinin, A. Jablonski, J. Zemek, and S. Hucek, J. Electron Spectrosc. Relat. Phenom. 87, 127 (1997).
- [26] A. Jablonski, F. Salvat, and C. J. Powell, J. Phys. Chem. Ref. Data 33, 409 (2004).
- [27] M. P. Seah and I. S. Gilmore, Surf. Interface Anal. 31, 835 (2001).
- [28] C. J. Powell and A. Jablonski, NIST Electron Effective-Attenuation-Length Database, SRD 82, Version 1.2 (2009); <http://www.nist.gov/ts/msd/srd/nist82.cfm>.
- [29] C. J. Powell, A. Jablonski, W. S. M. Werner, and W. Smekal, Appl. Surf. Science 239, 470 (2005).
- [30] NIST Database for the Simulation of Electron Spectra for Surface Analysis, SRD 100, Version 1.2 (2010); <http://www.nist.gov/ts/msd/srd/nist100.cfm>.
- [31] W. Smekal, W. S. M. Werner, and C. J. Powell, Surf. Interface Anal. 37, 1059 (2005).
- [32] C. J. Powell, W. S. M. Werner, W. Smekal, and G. Tasneem (to be published).